

Site Selectivity of Competitive Antagonists for the Mouse Adult Muscle Nicotinic Acetylcholine Receptor

Man Liu¹ and James P. Dilger

Department of Anesthesiology, Stony Brook University, Stony Brook, New York

Received August 4, 2008; accepted October 8, 2008

ABSTRACT

The muscle-type nicotinic acetylcholine receptor has two non-identical binding sites for ligands. The selectivity of acetylcholine and the competitive antagonists (+)-tubocurarine and metocurine for adult mouse receptors is known. Here, we examine the site selectivity for four other competitive antagonists: cisatracurium, pancuronium, vecuronium, and rocuronium. We rapidly applied acetylcholine to outside-out patches from transfected BOSC23 cells and measured macroscopic currents. We have reported the IC_{50} of the antagonists individually in prior publications. Here, we determined inhibition by pairs of competitive antagonists. At least one antagonist was present at a concentration producing $\geq 67\%$ receptor inhibition. Metocurine shifted the apparent IC_{50} of (+)-tubocurarine in quantitative agreement with complete competitive antagonism. The same was observed for pancuronium competing with vecuronium.

However, pancuronium and vecuronium each shifted the apparent IC_{50} of (+)-tubocurarine less than expected for complete competition but more than expected for independent binding. The situation was similar for cisatracurium and (+)-tubocurarine or metocurine. Cisatracurium did not shift the apparent IC_{50} of pancuronium or vecuronium, indicating independent binding of these two pairs. The data were fit to a two-site, two-antagonist model to determine the antagonist binding constants for each site, $L_{\alpha\epsilon}$ and $L_{\alpha\delta}$. We found $L_{\alpha\epsilon}/L_{\alpha\delta} = 0.22$ (range, 0.14–0.34), 20 (9–29), 21 (4–36), and 1.5 (0.3–2.9) for cisatracurium, pancuronium, vecuronium, and rocuronium, respectively. The wide range of $L_{\alpha\epsilon}/L_{\alpha\delta}$ for some antagonists may reflect experimental uncertainties in the low affinity site, relatively poor selectivity (rocuronium), or possibly that the binding of an antagonist at one site affects the affinity of the second site.

The nicotinic acetylcholine receptor (nAChR) is a prototypical member of a superfamily of pentameric ligand-gated ion channels, which includes muscle and neuronal nAChRs, 5-HT₃ receptors, GABA receptors, and glycine receptors (Unwin, 2005; Sine and Engel, 2006). The adult muscle type has the subunit stoichiometry $(\alpha 1)_2\beta 1\epsilon\delta$. This type of nAChR mediates rapid synaptic transmission at the neuromuscular junction. The binding of two molecules of ACh to sites in the extracellular domain promotes transmembrane cation channel opening. The two binding sites for ACh, situated between the $\alpha\epsilon$ - and $\alpha\delta$ -subunit interfaces of adult mouse nAChR, have similar affinities for ACh (Akk and Auerbach, 1996).

Antagonists such as (+)-tubocurarine and pancuronium compete with ACh for binding to these sites; the binding of a single antagonist is sufficient to prevent channel opening (see *Discussion*). Several competitive antagonists are known to distinguish between the two binding sites. The $\alpha\epsilon$ -interface has been identified as the high-affinity binding site for

(+)-tubocurarine and metocurine based on evidence from chimeras, mutations (Bren and Sine, 1997) and computational docking (Wang et al., 2003) in mouse or human nAChR. The affinity of the $\alpha\delta$ -interfacial site for these antagonists is 20–170-fold lower (Fletcher and Steinbach, 1996; Bren and Sine, 1997). There is less information about the site selectivity of other antagonists. Binding experiments have demonstrated that pancuronium and atracurium discriminate between the two sites in adult mouse nAChR by factors of 26 and 2.5, respectively (Fletcher and Steinbach, 1996). (Atracurium is a mixture of 10 stereoisomers; cisatracurium is the isomer that is currently used clinically). Vecuronium and cisatracurium are sensitive to mutations in the ϵ -subunit, whereas vecuronium, cisatracurium, and pancuronium are all sensitive to mutations in the δ -subunit (Dilger et al., 2007). These results suggest that antagonist combinations such as (+)-tubocurarine + vecuronium should not be completely competitive with each other and have a synergistic effect on inhibition. However, it has been reported that the inhibition produced by this combination in adult mouse nAChR is additive (Paul et al., 2002).

Here, we examine the site specificity of competitive antagonist binding to adult mouse nAChR measuring current in-

Supported by the National Institutes of Health [Grant NS045095].

¹ Current affiliation: Department of Medicine/Cardiology, University of Illinois at Chicago, Chicago, Illinois.

Article, publication date, and citation information can be found at <http://molpharm.aspetjournals.org>.
doi:10.1124/mol.108.051060.

ABBREVIATIONS: nAChR, nicotinic acetylcholine receptor; ECS, extracellular solution; ACh, acetylcholine.

hibition in the presence of pairs of antagonists. In contrast to the previous report (Paul et al., 2002), our measurements were made under conditions of high receptor inhibition by one or both antagonists. This provides a more sensitive test for synergistic effects (Waud and Waud, 1985; Nigrovic and Amann, 2004). We have used this approach in a study of adult human nAChR (Liu and Dilger, 2008) and found evidence for synergy; in some cases, synergy at the receptor level correlated with the clinical phenomenon of muscle relaxant synergy in which pairs of antagonist are more effective at inducing paralysis than expected from their individual potencies (Lebowitz et al., 1980; Waud and Waud, 1984).

Materials and Methods

Mouse adult muscle type nAChRs were expressed in BOSC23 cells (a subclone of human embryonic kidney 293 cells; American Type Culture Collection, Manassas, VA) using FuGENE 6 (Roche Diagnostics, Basel, Switzerland). Cells were prepared for patch-clamp recording as described before (Wenningmann and Dilger, 2001). Cells were transfected with cDNA coding for subunits of mouse adult muscle nAChR: α and β , wild type; ϵ , wild type, D59A, or D173N; δ , wild type, D180K [gifts of Dr. Steven Sine, Mayo Clinic, Rochester, MN (Ohno et al., 1996)] and for CD8 (gift of Dr. Brian Seed, Harvard Medical School, Cambridge, MA), a T-cell antigen used as a marker of transfected cells (Jurman et al., 1994). Experiments were performed on cells 2 to 4 days after transfection. Extracellular solution (ECS) contained 150 mM NaCl, 5.6 mM KCl, 1.8 mM CaCl₂, 1.0 mM MgCl₂, and 10 mM HEPES, pH 7.3. Transfected cells were identified by their affinity for polystyrene beads coated with a monoclonal antibody specific for the CD8 antigen (Dynabeads CD8; Invitrogen, Carlsbad, CA). Cells with two or more beads attached were considered likely to express nAChR as well as CD8 (Jurman et al., 1994).

Patch pipettes were filled with a solution consisting of 140 mM KCl, 5 mM EGTA, 5 mM MgCl₂, and 10 mM HEPES at pH 7.3, and had resistances of 2 to 7 M Ω . An outside-out patch (Hamill and Sakmann, 1981) with a seal resistance of ≥ 2 G Ω was excised from a cell and moved to a position at the outflow of a two-tube, gravity-driven, rapid perfusion system (HSSE-2; ALA Scientific Instruments, Westbury, NY). One tube contained ECS or ECS + antagonist—normal solution; the other contained ECS + 300 μ M ACh or ECS + 300 μ M ACh + antagonist—test solution. Manual valves were used to connect to reservoirs containing a defined concentration of antagonist with or without ACh. The patch was initially perfused with normal solution and exposed to the test solution for 0.25 s at 5-s intervals. An average of 6 to 20 responses, digitized at 100 μ s/point, was calculated. The perfusion system allowed a rapid exchange (~ 0.1 ms) of the solution bathing the patch (Liu and Dilger, 1991). Experiments were performed at room temperature, 22–25°C, and at a patch potential of -50 mV.

Acetylcholine chloride (purity >99%), (+)-tubocurarine chloride (purity 98%), pancuronium dibromide (purity >99%), HEPES, and EGTA were obtained from Sigma. Metocurine iodide was synthesized (King, 1935) from (+)-tubocurarine at the Chemical Synthesis Center, Department of Chemistry, Stony Brook University. Purity of 99% was determined by ¹H-NMR. Vecuronium bromide was obtained as the clinical formulation Norcuron from Bedford Labs, 1 mg/ml (1.8 mM) in a solution containing 2.1 mg/ml anhydrous citric acid, 1.6 mg/ml sodium phosphate, and 9.7 mg/ml mannitol. Dilutions were prepared in distilled water. The highest concentration of vecuronium used (1 μ M) contained 95 μ M mannitol. Rocuronium bromide was obtained as the clinical formulation Zemuron from Baxter Pharmaceutical Solutions LLC, 1 mg/ml (16.4 mM). Cisatracurium besylate was obtained as the clinical formulation Nimblex from GlaxoSmith-Kline, 2 mg/ml (2.1 mM) in a 35% benzene sulfonic acid solution. Dilutions were prepared in distilled water. The highest concentra-

tion of cisatracurium used, 1 μ M, contained 0.017% benzene sulfonic acid (1 mM).

When a single competitive antagonist was studied, currents were activated with 300 μ M ACh (a concentration that activates >95% of the channels) in the absence or presence of different concentrations of the antagonist. Inhibition is calculated as relative current, I_1/I_0 . I_0 and I_1 are the macroscopic peak currents measured in the absence and presence of antagonists, respectively. With some antagonists (e.g., metocurine, see Fig. 4), the current has a biphasic onset phase as a result of dissociation of antagonist on the 5- to 50-ms time scale and activation of previously antagonist-bound receptors. In this case, we use the current at the end of the rapid onset phase as representing the fraction of un-inhibited receptors before appreciable antagonist dissociation (Demazumder and Dilger, 2001; Dilger et al., 2007). The relative current versus concentration curve was fitted to a single site inhibition model by nonlinear least-squares regression using Prism 4.0c (GraphPad Software, San Diego, CA),

$$\frac{I_1}{I_0} = \frac{L}{L + c} \quad (1)$$

where c is the antagonist concentration and L is the dissociation equilibrium constant. We also fit the data to a two-site inhibition model,

$$\frac{I_1}{I_0} = \frac{L_{\alpha\epsilon}L_{\alpha\delta}}{L_{\alpha\epsilon}L_{\alpha\delta} + L_{\alpha\epsilon}c + L_{\alpha\delta}c + c^2} \quad (2)$$

where $L_{\alpha\epsilon}$ and $L_{\alpha\delta}$ are the dissociation constants for the α - ϵ and α - δ subunit interfaces, respectively. The model assumes that binding to one site is sufficient to inhibit channel opening. We used an F test to compare the two models. The two-site model was accepted if $p < 0.05$ (i.e., if the 95% confidence limits of $L_{\alpha\epsilon}$ and $L_{\alpha\delta}$ did not overlap).

Equation 3 gives the general expression for current inhibition by two antagonists binding at two sites.

$$\frac{I_{1+2}}{I_0} = \frac{1}{1 + \frac{c_1}{L_{\alpha\delta 1}} + \frac{c_1}{L_{\alpha\epsilon 1}} + \frac{c_1^2}{L_{\alpha\delta 1}L_{\alpha\epsilon 1}} + \frac{c_2}{L_{\alpha\delta 2}} + \frac{c_2}{L_{\alpha\epsilon 2}} + \frac{c_2^2}{L_{\alpha\delta 2}L_{\alpha\epsilon 2}} + \frac{c_1c_2}{L_{\alpha\delta 1}L_{\alpha\epsilon 2}} + \frac{c_1c_2}{L_{\alpha\delta 2}L_{\alpha\epsilon 1}}} \quad (3)$$

Here, we have distinguished the two antagonists by subscripts 1 and 2. When two antagonists were studied, the concentration-response curve for one antagonist was measured in the constant presence of a second antagonist at a concentration equal to 2 to 3 times its IC₅₀ (IC₅₀ = L from the single-site model). The inhibition was calculated as the relative current, I_{1+2}/I_1 , where I_{1+2} is the macroscopic current activated by 300 μ M ACh in the presence of two antagonists.

The expression for the relative current, I_{1+2}/I_1 , is completely defined by two parameters: $L_{\text{ratio}1} = L_{\alpha\epsilon}/L_{\alpha\delta 1}$ and $L_{\text{ratio}2} = L_{\alpha\epsilon}/L_{\alpha\delta 2}$. Consider two limiting cases. 1) The two antagonists inhibit the receptor independently; Fig. 1A, trace 1 (dashed line), illustrates this with $c_2 = 2 \times \text{IC}_{50,2}$; $L_{\text{ratio}1} = 1000$, indicating that antagonist1 binds primarily to the $\alpha\delta$ site; $L_{\text{ratio}2} = 0.001$, indicating that antagonist2 binds primarily to the $\alpha\epsilon$ site. There is no shift in the apparent IC₅₀ for antagonist 1 in the presence of antagonist 2 ($\text{IC}_{50,1,\text{app}} = \text{IC}_{50,1} = 1$ arbitrary concentration unit). 2) The two antagonists compete for a single site; the relative current is given by

$$\frac{I_{1+2}}{I_1} = \frac{1}{1 + c_1/\text{IC}_{50,1} + c_2/\text{IC}_{50,2}}$$

The apparent IC₅₀ of the first antagonist in the presence of the second antagonist is $\text{IC}_{50,1,\text{app}} = \text{IC}_{50,1}(1 + c_2/\text{IC}_{50,2})$. So, for $c_2 = 2$ or $3 \times \text{IC}_{50,2}$, the apparent IC₅₀ of the first antagonist will be 3- or 4-fold larger than its individual IC₅₀. In Fig. 1A, trace 4, $L_{\text{ratio}1} = L_{\text{ratio}2} = 1000$, indicating that both antagonists bind primarily to the $\alpha\delta$ site

and $IC_{50,1app}$ is shifted 3-fold to the right. Two other predictions of eq. 3 are presented as traces 2 and 3 in Fig. 1A. For trace 2, both antagonists have a 10-fold preference for one site over the other, but the preferences are for the opposite sites. There is a small, 1.3-fold shift in the curve. In contrast, if the antagonists have a 10-fold preference for the same site (the $\alpha\delta$ site in Fig. 1A Trace 3), the curve is shifted 2.25-fold. The contour plot in Fig. 1B summarizes many

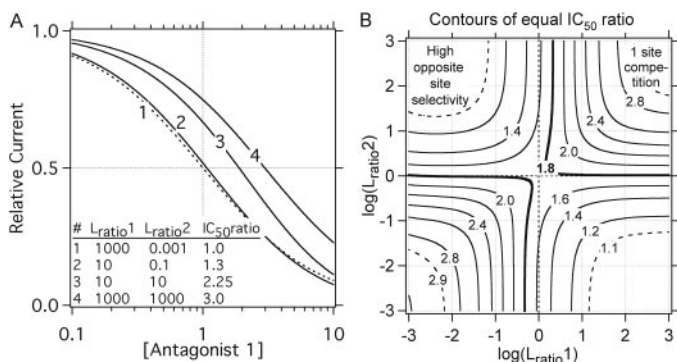


Fig. 1. Predictions of the two-antagonist, two-site model of eq. 3. A, examples of concentration-response curves predicted by eq. 3. The relative current is I_{1+2}/I_1 , the current seen in the presence of antagonist1 + a fixed concentration of antagonist2 compared with the current seen in the presence of antagonist1 alone. Antagonist1 alone is assumed to have $IC_{50} = 1$. The four curves are drawn for the indicated values of L_{ratio1} ($L_{\alpha\delta}/L_{\alpha\gamma}$) and L_{ratio2} ($L_{\alpha\delta}/L_{\alpha\gamma}$). Curve 1 is the dashed line. The IC_{50} ratios ($IC_{50,1app}/IC_{50,1}$), the shift in the IC_{50} antagonist1 caused by the presence of antagonist2 at $c_2 = 2 \times IC_{50,2}$. B, a contour plot illustrating the relationship between the IC_{50} ratio and each antagonist's selectivity for one site over the other. The contours are drawn assuming $c_2 = 2 \times IC_{50,2}$. The solid line contours are drawn at 0.2-unit intervals. The dashed line contours are at intermediate values. The contour plot has diagonal symmetry. The IC_{50} ratio is an indicator of the relative preference of the two antagonists for the two binding sites. When the ratio is close to 1.0, the antagonists prefer opposite sites and do not compete with each other. When the ratio is close to 1.8 (bold line), one or both antagonists bind equally well to both sites. When the ratio is close to 3.0, both antagonists compete for binding to the same site.

predictions of eq. 3 in terms of the IC_{50} ratio ($IC_{50,1app}/IC_{50,1}$) for different antagonist 1 and antagonist 2 L ratios with the assumption that $c_2 = 2 \times IC_{50,2}$. The contour plot has diagonal symmetry. When the two antagonists prefer the same site, $2 < IC_{50} ratio < 3$. When they prefer opposite sites, $1 < IC_{50} ratio < 1.8$.

We fit each trio of data sets (antagonist 1 alone, antagonist 2 alone, antagonist 1 in the presence of antagonist 2; a total of 90–100 data points) to the complete model (eq. 3) using multivariate, nonlinear regression to solve for the four equilibrium constants using the least-squares algorithm provided in IgorPro (version 6.03A; WaveMetrics, Inc., Lake Oswego, OR). The parameters were constrained to $0 < L < 30,000$ (nM) to avoid nonphysical solutions and to acknowledge that there are no data points above 1000 nM. After the algorithm converged on a solution, we reversed the high- and low-affinity equilibrium constants for one of the antagonists (this affects the fit to the paired antagonist data only) and used these as a seed for another fit determination. In all cases, the fitting routine returned the original solution. A parameter was considered to be indeterminate if a low-affinity constant reached 30,000 nM without converging.

Inhibition of mutant nAChR by rocuronium was determined at 40 nM rocuronium; a concentration corresponding to $2 \times IC_{50}$ of wild type receptors. We previously published similar data for the other antagonists (Dilger et al., 2007).

Results

Inhibition by Single Antagonists. We published IC_{50} values for the individual nondepolarizing competitive antagonists (+)-tubocurarine, metocurine, cisatracurium, pancuronium, and vecuronium on adult mouse nAChR (Dilger et al., 2007). Here, we include experiments with another clinically used drug, rocuronium. Rocuronium is an amino-steroid similar to pancuronium and vecuronium (Fig. 2). Figure 3A shows an example of macroscopic currents activated by rapid perfusion of 300 μ M ACh to an outside-out patch from a BOSC-23 cell transfected with adult mouse wild-type AChR. Inward currents, at -50 mV, rise to a peak within 300 μ s and

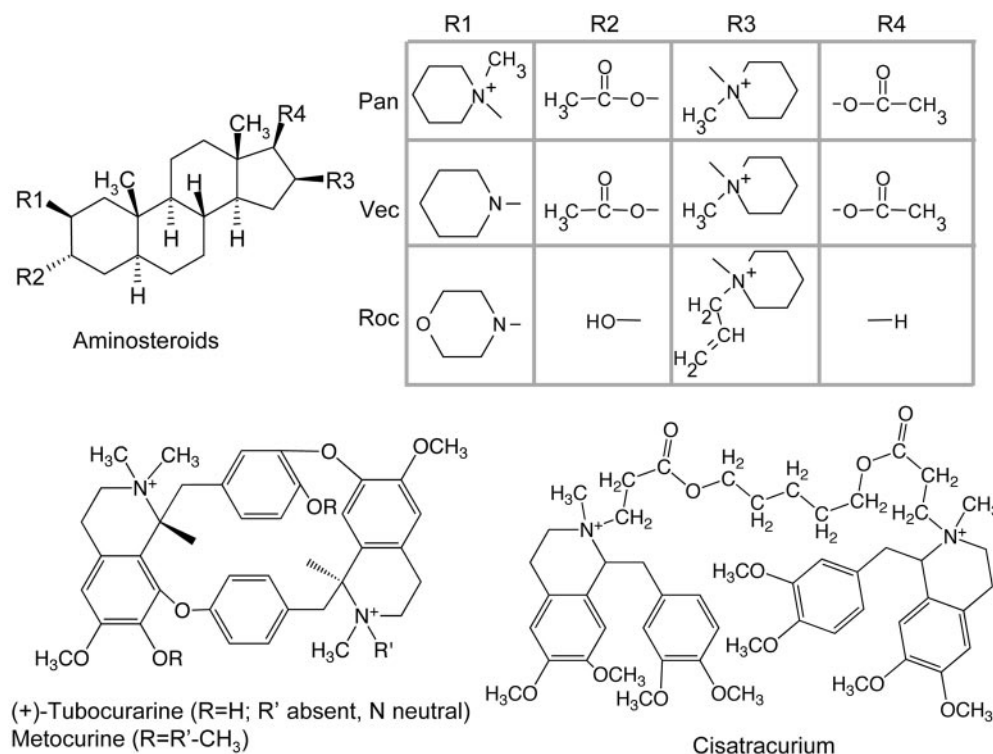


Fig. 2. The structures of the competitive antagonists used in this study.

decay as a result of desensitization (Dilger and Liu, 1992) with a time constant of approximately 30 ms. When 15 nM rocuronium is present before and during application of ACh, the peak current is reduced, but the time course of the current is unaltered. The reduced peak current corresponds to the number of channels that have not been inhibited by rocuronium. The relative peak currents for 3 to 300 nM rocuronium are shown in Fig. 3B along with the fit to the one-site inhibition model. For rocuronium, $L = 22 \pm 2$ nM (S.E.M.). The fit to the two-site inhibition model gave values of 34 ± 21 nM and 117 ± 156 nM. The F test for comparison of the models indicated that we should not reject the null hypothesis that the one-site model is preferable ($F_{1,28} = 1.77$, $p = 0.19$).

The IC_{50} values for all single-antagonist experiments are presented in Table 1. In most cases, the one-site model was not rejected by the F test. For cisatracurium, however, the two-site model was preferred (L values of 73 ± 11 and 400 ± 190 nM, $F_{1,38} = 14.1$, $p = 0.0006$) (Demazumder and Dilger, 2001).

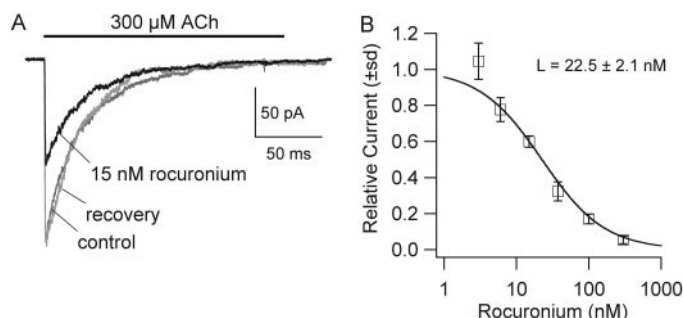


Fig. 3. Inhibition of adult, mouse nAChR by rocuronium. A, an example of macroscopic currents activated by 300 μ M ACh and inhibition by 15 nM rocuronium. B, the concentration-response curve for rocuronium. The L value was obtained by fitting the relative currents to a single binding site model. In this model, L is equivalent to the IC_{50} of the antagonist.

TABLE 1

Inhibition of adult, mouse nAChR by individual and pairs of competitive antagonists

IC_{50} values for antagonists applied alone and apparent IC_{50} values for combinations of antagonists. Ratio = $IC_{50,1app}/IC_{50,1}$. The "Pred ratio" column contains the IC_{50} ratios predicted from the equilibrium constants listed in Table 3. This serves as a test for overall self-consistency in the data because the values in Table 3 are averages from all experiments rather than the fit results from one pair of antagonists. In most cases, the predicted ratio falls within the 95% confidence limits of the experimental ratio. IC_{50} values for single antagonists were taken from our previous study (Dilger et al., 2007) with the exception of rocuronium.

| Antagonist 1 | Antagonist 2 | $IC_{50,1}$ (95% CL) | Ratio (95% CL) | Pred Ratio |
|-----------------|----------------------|----------------------|-------------------------------|------------------|
| <i>nM</i> | | | | |
| (+)tubocurarine | | 30.5 (27.1–34) | | |
| | 170 nM Metocurine | 108 (88–127) | 3.53 (2.78–4.28) ^a | 3.8 |
| | 110 nM Cisatracurium | 61.4 (49.7–73) | 2.01 (1.56–2.46) | 2.5 |
| | 30 nM Pancuronium | 43.8 (37.2–50.3) | 1.43 (1.16–1.7) | 1.1 ^b |
| | 40 nM Vecuronium | 50 (40.8–59.2) | 1.64 (1.28–1.99) | 1.1 ^b |
| Metocurine | 40 nM Rocuronium | 44.2 (36.4–52) | 1.45 (1.14–1.75) | 1.6 |
| | | 59.5 (50–69) | | |
| | 110 nM Cisatracurium | 128 (108–148) | 2.16 (1.67–2.64) | 2.5 |
| | 30 nM Pancuronium | 83.2 (63–103.4) | 1.4 (0.99–1.81) ^c | 1.1 |
| Cisatracurium | 40 nM Rocuronium | 64.1 (47.5–80.6) | 1.08 (0.75–1.4) ^c | 1.6 ^b |
| | | 53.8 (49.2–58.5) | | |
| Pancuronium | | 85.4 (65.8–105) | 1.59 (1.2–1.98) | 1.6 |
| | | 14.8 (12.6–16.9) | | |
| | 40 nM Rocuronium | 21.4 (18.6–24.1) | 1.45 (1.17–1.73) | 1.7 |
| Vecuronium | 110 nM Cisatracurium | 17.6 (15.4–19.9) | 1.19 (0.96–1.42) ^c | 1.3 |
| | | 20.4 (17.8–22.9) | | |
| | 30 nM Pancuronium | 69.1 (54.7–83.5) | 3.39 (2.57–4.22) ^a | 2.5 ^b |
| Rocuronium | 40 nM Rocuronium | 36 (30.4–41.7) | 1.77 (1.41–2.12) | 1.7 |
| | 110 nM Cisatracurium | 25 (21.4–28.6) | 1.23 (0.99–1.46) ^c | 1.3 |
| | | 22.5 (18.2–26.8) | | |

^a The 95% confidence limits of the ratio overlap 3–4 (consistent with competitive binding).

^b Predicted ratio does not fall within the 95% confidence limits of the experimental ratio.

^c The 95% confidence limits of the ratio overlap 1.0 (consistent with independent binding).

Inhibition by Pairs of Antagonists. With the knowledge of IC_{50} values of each individual antagonist, we performed combination experiments. We measured the concentration-response curve of an antagonist in the presence of a second antagonist at the concentration that inhibited $\geq 67\%$ of the receptors. The result was the apparent IC_{50} of the first antagonist, $IC_{50,1app}$. The results are illustrated in Figs. 4 to 6 and summarized in Table 1. Figure 4 shows the two combinations that produced inhibition in accord with competition for a single site. This is illustrated in the currents of Fig. 4A [inhibition by 200 nM (+)-tubocurarine alone] and Fig. 4B [inhibition by 200 nM (+)-tubocurarine in the presence of 170 nM metocurine]. The effectiveness of (+)-tubocurarine is reduced when metocurine is coapplied. This results in a rightward shift in the concentration-response curve of (+)-tubocurarine when 170 nM ($3 \times IC_{50}$) metocurine was present (Fig. 4C). A similar shift is seen for vecuronium when 30 nM ($2 \times IC_{50}$) pancuronium was used (Fig. 4D). Table 1 shows that the 95% confidence intervals for $IC_{50,1app}/IC_{50,1}$ overlap the values predicted for competitive binding to the same site (4.0 for (+)-tubocurarine + metocurine, 3.0 for vecuronium + pancuronium).

Figure 5 shows that there is no change in the apparent IC_{50} of pancuronium when 110 nM ($2 \times IC_{50}$) cisatracurium is present. This suggests that the two antagonists bind independently. The 95% confidence limits of $IC_{50,1app}/IC_{50,1}$ for this and three other combinations overlap 1.0 as indicated in Table 1. In agreement with this, an F test assessing the difference between the pancuronium and pancuronium + cisatracurium data sets concluded that there is no significant difference ($F_{1,58} = 3.57$, $p = 0.064$).

Figure 6 presents two of the eight combinations of antagonists that could not be identified as either competing for a single site or inhibiting the nAChR independently. Forty nanomolar ($2 \times IC_{50}$) vecuronium caused a 1.64-fold shift in

the concentration response curve of (+)-tubocurarine (Fig. 6A) and 40 nM rocuronium ($2 \times IC_{50}$) produced a 1.77-fold shift in the curve of vecuronium (Fig. 6B). *F* tests comparing the pairs of data sets indicate that they are significantly different from each other ($F_{1,69} = 21.2$, $p < 0.0001$ for (+)-tubocurarine/pancuronium; $F_{1,41} = 35.1$, $p < 0.0001$ for vecuronium/rocuronium). Table 1 shows that the IC_{50} ratios for these eight combinations ranged from 1.4 to 2.2 and the 95% confidence limits did not overlap either 1.0 or 3.0.

We then analyzed the data considering the complete model for two antagonists binding to two sites (eq. 3). For each pair of antagonists, we simultaneously fit three inhibition curves (each antagonist separately and both antagonists together) to eq. 3 with both antagonist concentrations as independent variables. The resulting estimates of binding constants are shown in Table 2 along with 95% confidence limits. Because it has already been shown that (+)-tubocurarine binds much more strongly to the $\alpha\epsilon$ interface than to the $\alpha\delta$ interface (Wang et al., 2003), we examined this antagonist with each of the others. In addition, as expected from previous work (Bren and Sine, 1997; Wang et al., 2003) and from Fig. 4A, the $\alpha\epsilon$ interface is also the high-affinity site for metocurine. The estimates for the affinity of (+)-tubocurarine to the $\alpha\delta$ interface converge in the fitting routine, but the confidence limits are larger than the values themselves; this is due to the absence of data at >300 nM concentrations. For, metocurine, the $L_{\alpha\delta}$ estimates did not converge, reflecting the high

selectivity of this antagonist. For combinations of (+)-tubocurarine and the other antagonists, we found that cisatracurium binds more tightly to the $\alpha\epsilon$ interface, whereas pancuronium, vecuronium, and rocuronium all bind more tightly to the $\alpha\delta$ interface. Pancuronium and vecuronium are highly selective but rocuronium is much less selective. The identification of the high-affinity site for the (+)-tubocurarine + antagonist data were used for the remaining fits listed in Table 2.

Table 3 summarizes the data for each antagonist and includes the selectivity ratio, $L_{\alpha\epsilon}/L_{\alpha\delta}$. The results consistently show that cisatracurium has a 4.5-fold preference for the $\alpha\epsilon$ interface; pancuronium and vecuronium have a high, but variable preference for the $\alpha\delta$ interface; and rocuronium binds to both sites with similar affinity. The large range in some of the parameters in Table 3 is due to the large uncertainties in determining the low-affinity binding constants.

Inhibition of Other Receptor Constructs by Rocuronium. To supplement our previous data with the other antagonists (Dilger et al., 2007), we measured inhibition by 40 nM rocuronium ($2 \times IC_{50}$) on some mutant adult mouse receptors and receptors with two δ -subunits. This concentration decreases currents in wild-type receptors to 0.32 ± 0.05 of control. Receptors containing a mutation at either of two sites in the ϵ -subunit, $\epsilon D59A$ or $\epsilon D173N$, are known to decrease the binding of (+)-tubocurarine and metocurine (Bren and Sine, 1997; Wang et al., 2003). Rocuronium was also

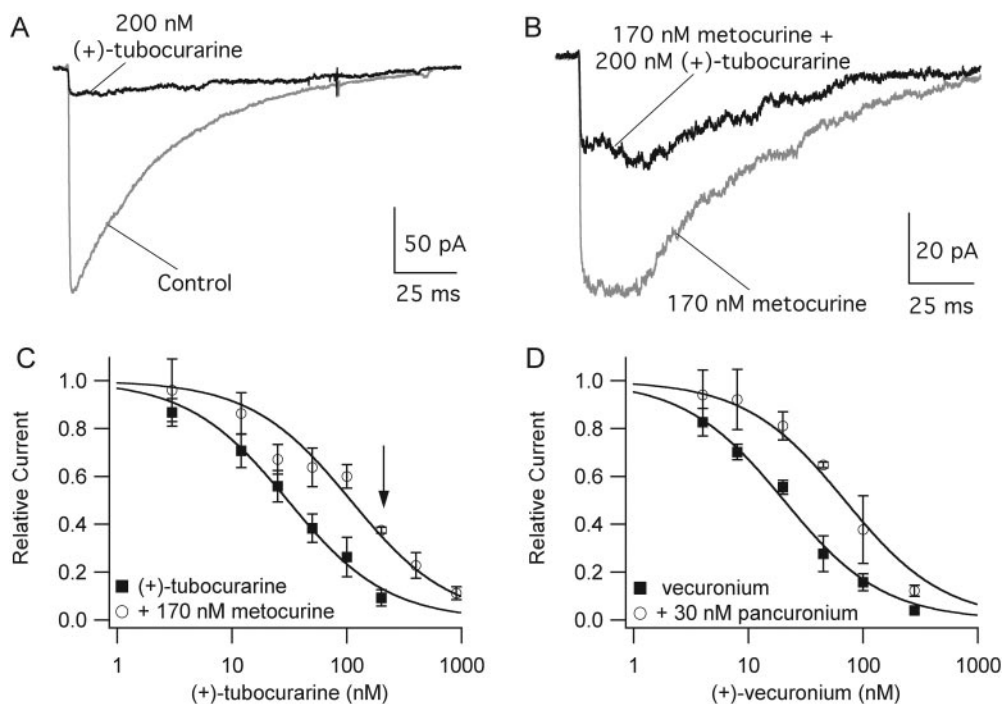


Fig. 4. Antagonists that compete for the same high-affinity binding site in adult mouse nAChR. Relative currents in the presence of a single antagonist and the same antagonist in the presence of a constant concentration of a second antagonist. The latter is normalized to the current amplitudes in the presence of the second antagonist alone (approximately 70% inhibition of antagonist-free control). A, an example from an experiment using one antagonist only. ACh (300 μ M) is used to activate currents. (+)-Tubocurarine (200 nM) decreased the peak current to 0.12 of control. B, an example from a different patch showing inhibition by 200 nM (+)-tubocurarine in the presence of 170 nM metocurine. (+)-Tubocurarine (200 nM) decreased the initial peak current to 0.39 of that produced in the presence of 170 nM metocurine alone. This is considerably less inhibition than is produced by 200 nM (+)-tubocurarine alone. Note that metocurine causes the ACh activated currents to have a biphasic onset and truncated peak as a result of the dissociation of metocurine from receptors on the 10-ms timescale (see *Materials and Methods*). C, (+)-tubocurarine and metocurine compete for the antagonist binding site at the $\alpha\epsilon$ -subunit interface. The 3.5-fold shift in the apparent IC_{50} of (+)-tubocurarine when 170 nM metocurine ($3 \times$ the IC_{50} of metocurine) is present, is consistent with competition for a single site. The arrow indicates 200 nM (+)-tubocurarine, the concentration used for the data in parts A and B. D, vecuronium and pancuronium seem to compete for a single site as evidenced by the 3.4-fold shift in the apparent IC_{50} of vecuronium when 30 nM pancuronium ($2 \times IC_{50}$) is present.

sensitive to these mutations: currents in the presence of 40 nM rocuronium were 0.45 ± 0.07 ($p = 0.004$) and 0.43 ± 0.04 ($p = 0.001$) of control, respectively. A mutation in the δ -subunit, δ D180K, has been shown to decrease binding of (+)-tubocurarine to mouse nAChR with two copies of the δ -subunit (Martin and Karlin, 1997). Inhibition by rocuronium of $\alpha_2\beta\epsilon\delta$ (D180K) receptors was also decreased; 40 nM rocuronium reduced currents to 0.70 ± 0.08 of control ($p = 0.0002$). Finally, we expressed receptors with two copies of the wild-type δ -subunit (lacking the ϵ -subunit). Inhibition by rocuronium was enhanced such that 40 nM rocuronium decreased currents to 0.16 ± 0.01 of control ($p = 0.008$). We found no evidence for functional channels in cells transfected with cDNA for the α , β and ϵ -subunits only.

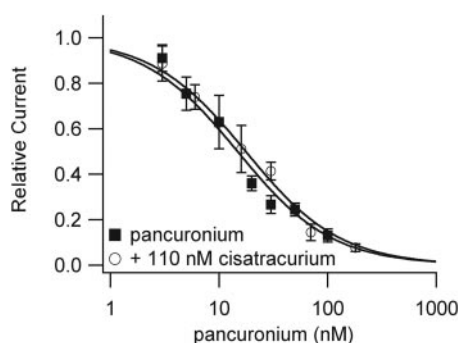


Fig. 5. Pancuronium and cisatracurium inhibit independently. There is no significant difference between the apparent IC_{50} of pancuronium when 110 nM cisatracurium is present. This suggests that the two drugs bind primarily to different sites.

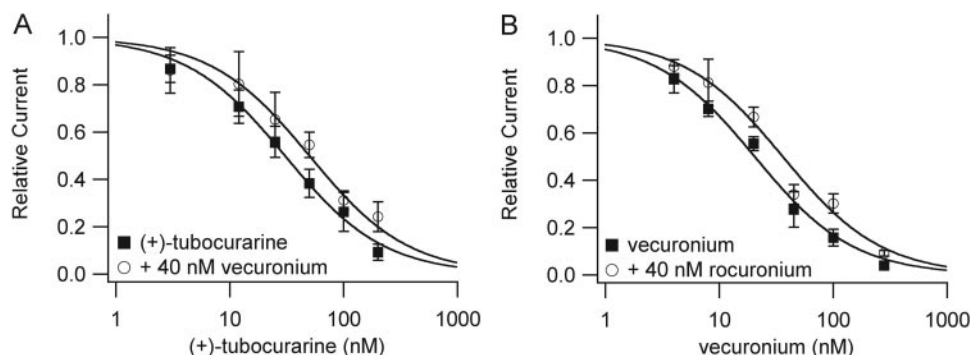


Fig. 6. Antagonist combinations producing intermediate shifts in apparent IC_{50} . A, (+)-tubocurarine + vecuronium. The apparent IC_{50} is shifted 1.64-fold (Table 1). B, vecuronium + rocuronium. The apparent IC_{50} is shifted 1.77-fold (Table 1).

TABLE 2

Results of fitting the inhibition data to a two-site, two-drug model

The results of fitting complete data sets (antagonists 1 and 2 separately and the pair of antagonists) to a two-site, two-drug inhibition model (eq. 3). With metocurine, there was no convergence for $L_{\alpha\delta}$; fitting process was halted when $L_{\alpha\delta} = 30,000$ nM. In all other cases, after convergence was reached, the $L_{\alpha\epsilon}$ and $L_{\alpha\delta}$ values of antagonist 2 were reversed and used as seeds for a second fit. The results were the same as for the initial fit.

| Antagonist 1 | $L_{\alpha\epsilon}$ (95% CL) | $L_{\alpha\delta}$ (95% CL) | Antagonist 2 | $L_{\alpha\epsilon}$ (95% CL) | $L_{\alpha\delta}$ (95% CL) |
|-----------------|-------------------------------|-----------------------------|---------------|-------------------------------|-----------------------------|
| | nM | | | nM | |
| (+)Tubocurarine | 31 (3) | 7700 (44000) | Metocurine | 58 (7) | |
| | 31 (2) | 5900 (30000) | Cisatracurium | 85 (20) | 250 (110) |
| | 32 (3) | 2500 (7500) | Pancuronium | 170 (120) | 18 (3) |
| | 32 (3) | 2600 (7500) | Vecuronium | 120 (80) | 29 (7) |
| | 31 (4) | 3800 (19000) | Rocuronium | 82 (58) | 39 (16) |
| Metocurine | 60 (5) | | Cisatracurium | 81 (17) | 280 (120) |
| | 60 (8) | | Pancuronium | 200 (200) | 18 (3) |
| | 59 (8) | | Rocuronium | 99 (84) | 34 (13) |
| Cisatracurium | 70 (14) | 460 (320) | Rocuronium | 54 (58) | 55 (57) |
| Pancuronium | 300 (380) | 17 (3) | Rocuronium | 35 (13) | 110 (100) |
| | 380 (350) | 16 (2) | Cisatracurium | 69 (9) | 490 (240) |
| Vecuronium | 800 (1000) | 22 (2) | Pancuronium | 610 (910) | 16 (2) |
| | 500 (770) | 23 (4) | Rocuronium | 59 (42) | 52 (37) |
| | 520 (490) | 22 (2) | Cisatracurium | 70 (9) | 440 (180) |

2007). In this article, we revisit this question by studying inhibition of adult mouse nAChR in outside-out patches by pairs of antagonists under conditions of $\geq 67\%$ current inhibition.

We (and others) assumed that binding of a competitive antagonist to one of the sites was sufficient to inhibit ACh-activated currents. ACh can activate channels when bound to only one site, but the rate of opening of monoliganded receptors in adult mouse AChR is 250-fold lower than for diliganded receptors (Wang et al., 1997). Fletcher and Steinbach (1996) showed that in adult mouse AChR, neither (+)-tubocurarine, metocurine, pancuronium, nor atracurium activates channels directly and found no evidence for gating by heteroliganded receptors. They also found that functional block was correlated to high-affinity binding, and this implies that occupation of a single site is sufficient for full functional block. Studies of heteroliganded openings with ACh and partial agonists such as decamethonium (Liu and Dilger, 1993) or choline (Purohit and Grosman, 2006) indicate that heteroliganded channels open at a slower rate than diliganded (ACh) channels. Because our assessment of antagonist inhibition is made within 1 ms of agonist application, it is unlikely that heteroliganded receptors make a significant contribution.

In our experiments, one antagonist was present at a concentration 2 to 3 times its individual IC_{50} . Under these conditions, the apparent IC_{50} of another antagonist would be shifted to 3- to 4-fold higher concentrations if both drugs were competing for a single site. This was the case for two of the 14 combinations we examined: (+)-tubocurarine + metocurine and pancuronium + vecuronium (Fig. 4, Table 1). The former result agrees with previous determinations that (+)-tubocurarine and metocurine are both selective for the $\alpha\text{-}\epsilon$ interfacial site (Bren and Sine, 1997; Wang et al., 2003). The latter result is in agreement with the study by Paul et al. (2002), who also reported additivity with the pancuronium + vecuronium combination. We found four combinations of antagonists for which there was no significant shift in apparent IC_{50} (Fig. 5, Table 1). However, it should be noted that for these combinations, the 95% confidence intervals of the IC_{50} ratios were large; further experiments might show evidence for a ratio significantly different from 1. The remaining eight combinations have IC_{50} ratios that are intermediate between 1.0 and 3 and 4. This includes (+)-tubocurarine + pancuronium, a pair that was examined by Paul et al. (2002) and was determined by them to be additive. Based on our value of 1.4 for the IC_{50} ratio, it would be very difficult to see evidence for superadditivity under the conditions of low receptor occupancy used by Paul et al. (2002).

TABLE 3

A summary of the fit parameters from Table 2

The table displays the average values and ranges of the parameters obtained from the four or five (n) sets of paired antagonist data. Values are presented as mean \pm S.D.

| Antagonist | n | $L_{\alpha\epsilon}$ | $L_{\alpha\delta}$ | $L_{\alpha\epsilon}/L_{\alpha\delta}$ (range) |
|------------------|-----|----------------------|--------------------|---|
| <i>nM</i> | | | | |
| (+)-Tubocurarine | 5 | 31 ± 1 | 4500 ± 2200 | 0.008 (0.004–0.012) |
| Metocurine | 4 | 59 ± 1 | | |
| Cisatracurium | 5 | 75 ± 8 | 380 ± 110 | 0.22 (0.14–0.34) |
| Pancuronium | 5 | 330 ± 180 | 17 ± 1 | 20 (9–29) |
| Vecuronium | 4 | 480 ± 280 | 24 ± 3 | 21 (4–36) |
| Rocuronium | 5 | 66 ± 25 | 59 ± 32 | 1.5 (0.3–2.9) |

We then took the approach of fitting all of the data for a given combination of antagonists (each antagonist alone and the combination) to eq. 1 to estimate the binding constants for each antagonist at each site. The results, presented in Table 2, show a general consistency among the data sets. In particular, 1) the benzyloisoquinoliniums have a higher affinity for the $\alpha\text{-}\epsilon$ site than for the $\alpha\text{-}\delta$ site, 2) two of the aminosteroids (pancuronium and vecuronium) have a higher affinity for the $\alpha\text{-}\delta$ site than for the $\alpha\text{-}\epsilon$ site, and 3) rocuronium has very similar affinity for both sites. Quantitatively, the uncertainties in the low-affinity values are very large, sometimes as large as the values themselves. This is because of paucity of data at high antagonist concentrations; this is a limitation for any functional measures of inhibition. With rocuronium, the similarity of the two affinities leads to large uncertainties in both parameters. The individual results for each data set are combined to give overall averages for the site specificity of each antagonist in Table 3. In agreement with published data, (+)-tubocurarine and metocurine are both very specific for the $\alpha\text{-}\epsilon$ interface although the $L_{\alpha\epsilon}/L_{\alpha\delta}$ estimates determined here [1/250–1/83 for (+)-tubocurarine, <1/5000 for metocurine] are more different from 1.0 than in published data [1/17 for (+)-tubocurarine (Fletcher and Steinbach, 1996), 1/170 for metocurine (Bren and Sine, 1997)]. Cisatracurium is not monogamous like the other benzyloisoquinoliniums but still favors the $\alpha\text{-}\epsilon$ interface by a factor of 3 to 7; this ratio is similar to that found for the stereoisomeric mixture atracurium, 2.5 (Fletcher and Steinbach, 1996). The 9- to 29-fold preference of pancuronium for the $\alpha\text{-}\delta$ -interface found here is in good agreement with the published result of binding experiments, 26-fold (Fletcher and Steinbach, 1996). Although vecuronium has a site selectivity similar to that of pancuronium, rocuronium shows very little preference between the sites. This is also evident from our finding that mutations in both the ϵ - and δ -subunits affect the inhibitory potency of rocuronium.

Finally, we used the average values of affinities from Table 3 to predict the shift in apparent IC_{50} for each of the combinations and included this in the last column of Table 1. This analysis, without any attempt at determining error ranges, serves as a way to assess the self-consistency of all of our data sets. The predicted IC_{50} ratios are within the 95% confidence intervals of the experimental values in 10 of the 14 cases. The small deviations may be due to receptor inhomogeneity, to a lack of data at high antagonist concentrations, or to interactions between the sites. For example, binding of (+)-tubocurarine at one site might decrease the affinity for binding of pancuronium at the other site. We have previously discussed

TABLE 4

A summary of the fit parameters for adult human AChR data

Previously published one- and two- antagonist inhibition data for adult human nAChR (Liu and Dilger, 2008) were fitted to eq. 3 using the same approach that was used for adult mouse nAChR (Table 3). Because the Hill slope of the rocuronium (alone) data on adult human nAChR was small (0.67), the fits to eq. 3 did not converge. Thus, rocuronium is not included in the table. Values are presented as mean \pm S.D.

| Antagonist | n | $L_{\alpha\epsilon}$ | $L_{\alpha\delta}$ | $L_{\alpha\epsilon}/L_{\alpha\delta}$ (range) |
|------------------|-----|----------------------|--------------------|---|
| <i>nM</i> | | | | |
| (+)-Tubocurarine | 4 | 25.6 ± 0.3 | | |
| Metocurine | 3 | 22 ± 2 | 340 ± 200 | 0.08 (0.04–0.11) |
| Cisatracurium | 4 | 13 ± 1 | 260 ± 170 | 0.07 (0.02–0.11) |
| Pancuronium | 4 | | 6.4 ± 0.1 | |
| Vecuronium | 3 | 500 ± 320 | 17 ± 2 | 30 (14–46) |

the evidence in favor of conformational changes in the nAChR induced by binding of competitive antagonists (Demazumder and Dilger, 2008).

In our previous article (Liu and Dilger, 2008), we measured inhibition of adult human nAChR in the presence of one or two antagonists. An analysis of this data in terms of eq. 3 is presented in Table 4. We assumed that the α - ϵ interface was the high-affinity site for (+)-tubocurarine (Wang et al., 2003). Although there are significant differences in the L values themselves, the site selectivity of antagonists for adult mouse (Table 3) and adult human (Table 4) is quite similar. Both metocurine and cisatracurium have higher affinities for the α - ϵ interface and both pancuronium and vecuronium favor the α - δ interface. (We were unable to determine the selectivity of rocuronium for adult human nAChR.)

The investigation by Paul et al. (2002) also examined combinations, including the competitive nAChR antagonist gallamine, which has three quaternary ammonium groups. We did not include gallamine in our study because we have found that it dissociates from the receptor within 1 ms, making it difficult to determine the degree of channel inhibition in our experiments (Demazumder, 2002).

It would be interesting to understand what difference in the structure of the amino-steroids pancuronium and rocuronium is responsible for one drug being highly selective for the α - δ interfacial binding site and the other drug not discriminating between the sites. It is difficult to speculate on this with only the currently available data. We plan to examine this using a computational chemistry approach. Differences in site-selectivity among analogs of (+)-tubocurarine for embryonic mouse and *Torpedo* spp. AChR have been previously noted: unlike (+)-tubocurarine and metocurine, which strongly favor one site over the other, *O,O*-dimethyl-tubocurarine does not discriminate between the sites (Papineni and Pedersen, 1997).

Here, we were able to determine the relative selectivity of an antagonist at two binding sites by measuring the inhibition induced by a mixture of this antagonist with an antagonist of known selectivity [(+)-tubocurarine]. This approach circumvents some of the problems that can arise from using mutagenesis to determine site selectivity (Dilger et al., 2007; Liu and Dilger, 2008) and may have more general applicability to other ligand-gated ion channels.

References

- Akk G and Auerbach A (1996) Inorganic, monovalent cations compete with agonists for the transmitter binding site of nicotinic acetylcholine receptors. *Biophys J* **70**:2652–2658.
- Bren N and Sine SM (1997) Identification of residues in the adult nicotinic acetylcholine receptor that confer selectivity for curariform antagonists. *J Biol Chem* **272**:30793–30798.
- Demazumder D (2002) The kinetics of competitive antagonism of nicotinic acetylcholine receptors. PhD thesis, State University of New York at Stony Brook, New York.

- Demazumder D and Dilger JP (2001) The kinetics of competitive antagonism by cisatracurium of embryonic and adult nicotinic acetylcholine receptors. *Mol Pharmacol* **60**:797–807.
- Demazumder D and Dilger JP (2008) The kinetics of competitive antagonism of nicotinic acetylcholine receptors at physiological temperature. *J Physiol* **586**:951–963.
- Dilger JP and Liu Y (1992) Desensitization of acetylcholine receptors in BC3H-1 cells. *Pflugers Arch* **420**:479–485.
- Dilger JP, Vidal AM, Liu M, Mettewie C, Suzuki T, Pham A, and Demazumder D (2007) Roles of amino acids and subunits in determining the inhibition of nicotinic acetylcholine receptors by competitive antagonists. *Anesthesiology* **106**:1186–1195.
- Fletcher GH and Steinbach JH (1996) Ability of nondepolarizing neuromuscular blocking drugs to act as partial agonists at fetal and adult mouse muscle nicotinic receptors. *Mol Pharmacol* **49**:938–947.
- Hamill OP and Sakmann B (1981) Multiple conductance states of single acetylcholine receptor channels in embryonic muscle cells. *Nature* **294**:462–464, 1981.
- Jurman ME, Boland LM, Liu Y, and Yellen G (1994) Visual identification of individual transfected cells for electrophysiology using antibody-coated beads. *Biotechniques* **17**:876–881.
- King H (1935) Curare alkaloids. Part I. Tubocurarine. *J Chem Soc* **57**:1381–1389.
- Lebowitz PW, Ramsey FM, Savarese JJ, and Ali HH (1980) Potentiation of neuromuscular blockade in man produced by combinations of pancuronium and metocurine or pancuronium and d-tubocurarine. *Anesth Analg* **59**:604–609.
- Liu M and Dilger JP (2008) Synergy between pairs of competitive antagonists at adult human muscle acetylcholine receptors. *Anesth Analg* **107**:525–533.
- Liu Y and Dilger JP (1991) Opening rate of acetylcholine receptor channels. *Biophys J* **60**:424–432.
- Liu Y and Dilger JP (1993) Decamethonium is a partial agonist at the nicotinic acetylcholine receptor. *Synapse* **13**:57–62.
- Martin MD and Karlin A (1997) Functional effects on the acetylcholine receptor of multiple mutations of gamma Asp174 and delta Asp180. *Biochemistry* **36**:10742–10750.
- Nigrovic V and Amann A (2004) Simulation of interaction between two non-depolarizing muscle relaxants: generation of an additive or a supra-additive neuromuscular block. *J Pharmacokinet Pharmacodyn* **31**:157–179.
- Ohno K, Wang HL, Milone M, Bren N, Brengman JM, Nakano S, Quiram P, Pruitt JN, Sine SM, and Engel AG (1996) Congenital myasthenic syndrome caused by decreased agonist binding affinity due to a mutation in the acetylcholine receptor epsilon subunit. *Neuron* **17**:157–170.
- Papineni RV and Pedersen SE (1997) Interaction of d-tubocurarine analogs with the mouse nicotinic acetylcholine receptor. Ligand orientation at the binding site. *J Biol Chem* **272**:24891–24898.
- Paul M, Kindler CH, Fokt RM, Dipp NC, and Yost CS (2002) Isobolographic analysis of non-depolarizing muscle relaxant interactions at their receptor site. *Eur J Pharmacol* **438**:35–43.
- Purohit Y and Grosman C (2006) Estimating binding affinities of the nicotinic receptor for low-efficacy ligands using mixtures of agonists and two-dimensional concentration-response relationships. *J Gen Physiol* **127**:719–735.
- Sine SM and Engel AG (2006) Recent advances in Cys-loop receptor structure and function. *Nature* **440**:448–455, 2006.
- Unwin N (2005) Refined structure of the nicotinic acetylcholine receptor at 4 Å resolution. *J Mol Biol* **346**:967–989.
- Wang HL, Auerbach A, Bren N, Ohno K, Engel AG, and Sine SM (1997) Mutation in the M1 domain of the acetylcholine receptor alpha subunit decreases the rate of agonist dissociation. *J Gen Physiol* **109**:757–766.
- Wang HL, Gao F, Bren N, and Sine SM (2003) Curariform antagonists bind in different orientations to the nicotinic receptor ligand binding domain. *J Biol Chem* **278**:32284–32291.
- Waud BE and Waud DR (1984) Quantitative examination of the interaction of competitive neuromuscular blocking agents on the indirectly elicited muscle twitch. *Anesthesiology* **61**:420–427.
- Waud BE and Waud DR (1985) Interaction among agents that block end-plate depolarization competitively. *Anesthesiology* **63**:4–15.
- Wenningmann I and Dilger JP (2001) The kinetics of inhibition of nicotinic acetylcholine receptors by (+)-tubocurarine and pancuronium. *Mol Pharmacol* **60**:790–796.

Address correspondence to: James P. Dilger, Department of Anesthesiology, Stony Brook University, Stony Brook, NY 11790-8480. E-mail: james.dilger@stonybrook.edu